Prisma Sains: Jurnal Pengkajian Ilmu dan Pembelajaran Matematika dan IPA IKIP Mataram
https://e-journal.undikma.ac.id/index.php/prismasains/index
e-mail: prismasains.pkpsm@gmail.com

January 2026. Vol. 14, No. 1
p-ISSN: 2338-4530
e-ISSN: 2540-7899
pp. 258-275

HVSR-Based Microzonation of Natural Frequency, Amplification, Vulnerability Index, and Ground Shear-Strain in Malang City, East Java

[1]Adedio Daniel Situmeang, [1]M. Rizky Saputra, [1]Yuansyah Dhaniar Ramdhan, [1]Safira Nur Cholisatin, [1]Divana Zumrotul Asyfiya, [1]Madlazim, [1]Muhammad Nurul Fahmi, [2]Alif Haidar Safrian, [2]Rasamala I.W Putri, [1*]Arie Realita

[1]Physics Study Program, Faculty of Mathematics and Natural Sciences, Surabaya State University, Indonesia

[2]Regional Disaster Management Agency of East Java Province, Indonesia

*Corresponding Author e-mail: arierealita@unesa.ac.id

Received: October 2025; Revised: December 2025; Published: January 2026

Abstract

Seismic activity in Malang City is very high due to tectonic dynamics in the subduction zone between the Indian-Australian and Eurasian plates and the active local faultsm, including the northeast-southwest trending Watukosek Fault, and the east-west fault around the Pasuruan Fault, which have the potential to cause damaging ground shaking in Malang City. The BMKG also recorded an earthquake with a magnitude of 4.5 Mw on March 16, 2025. Based on these events, this study was conducted to analyze the vulnerability of Malang City, East Java, using the Horizontal-Vertical Spectral Ratio (HVSR) method by integrating the parameters of natural frequency (f_0), amplification (Ag), soil vulnerability index (Kg), and Ground Shear-Strain (γ). A total of 19 points were processed using Geopsy software to obtain the HVSR curve and obtain the f_0 and Ag values, while Kg and γ were obtained from processing the HVSR parameters and then mapped through spatial interpolation in ArcGIS. The results of data processing and analysis show that several points in Malang City have f0 1.448 - 9.938 Hz with amplification 1.704 - 6.639 and soil vulnerability index values 0.383 - 14.871, as well as shear strain values up to 0.009. Zones are mainly concentrated by high amplification and vulnerability are mainly concentrated in the northern part of Kedungkandang District, the eastern part of Blimbing District, and parts of Lowokwaru District, which are dominated by higher frequencies with low amplification, as well as the western part of Sukun District, indicating a high level of earthquake risk. While previous studies primarily utilized only utilized natural frequencies and amplification, whereas this study offers HVSR-based microzonation by integrating dynamic soil parameters (f_0, Ag, Kg, and γ).

Keywords: Earthquake mitigation; HVSR, Malang City; Microzonation; Soil Vulnerability

How to Cite: Situmeang, A. D., Saputra, M. R., Ramadhan, Y. D., Cholisatin, S. N., Asyfiya, D. Z., Madlazim, M., … Realita, A. (2026). HVSR-Based Microzonation of Natural Frequency, Amplification, Vulnerability Index, and Ground Shear-Strain in Malang City, East Java. *Prisma Sains : Jurnal Pengkajian Ilmu Dan Pembelajaran Matematika Dan IPA IKIP Mataram*, *14*(1), 258–275. https://doi.org/10.33394/j-ps.v14i1.17820

https://doi.org/10.33394/j-ps.v14i1.17820

Copyright© 2026, Situmeang et al.
This is an open-access article under the CC-BY License.

INTRODUCTION

Malang City is situated in a tectonically active region of East Java and is exposed to considerable seismic hazard. On 16 March 2025, an Mw 4.5 earthquake struck the Malang area and was felt widely across the city, triggered public concern despite its moderate magnitude. The spatially variable intensity of shaking observed during this event indicates heterogeneous local site responses, which are strongly influenced by subsurface geological structure, lithology, and near-surface soil conditions that control seismic-wave amplification (Susilo et al., 2023).

Geographically, Malang City is located between 112°06′–112°07′ E and 7°06′–8°02′ S, covering an area of approximately 110.06 km² with elevations ranging from 440 to 667 m above sea level. From a regional geological perspective, the area is affected by the subduction

of the Indo-Australian Plate beneath the Eurasian Plate with a slab dip of about 49°–56° (Muttaqy et al., 2023). Seismic activity is further controlled by active local fault systems, notably the northeast–southwest–trending Watukosek Fault and the east–west–trending Pasuruan Fault, which cut Miocene to Quaternary formations (Iswanto, 2021). The interaction between regional subduction processes and local faulting generates a complex stress regime that can enhance ground-motion amplification in areas underlain by unconsolidated or heterogeneous sediments.

Microtremor surveys provide a non-destructive and cost-effective approach for characterizing near-surface soil dynamics related to seismic response (Gosar, 2017; Hernanti et al., 2014). The Horizontal-to-Vertical Spectral Ratio (HVSR) method, based on three-component ambient vibration recordings, is widely applied to estimate site fundamental frequency (f_0) and related parameters by analyzing the ratio between horizontal and vertical spectral amplitudes (Nakamura, 2008; Ridwan et al., 2019). Since microtremor signals are dominated by shear-wave resonance, HVSR-derived parameters such as f_0, amplification factor (A_0), vulnerability index (Kg), and seismic vulnerability parameter (γ) have been extensively used for seismic microzonation and urban planning in various geological settings (Maklad et al., 2020; Nagamani et al., 2020).

However, quantitative site-response characterization for Malang City remains limited, particularly in terms of city-scale spatial coverage and integrated interpretation of geological, morphological, and HVSR-derived parameters. While similar combinations of f_0, A_0, Kg, and γ have been successfully applied elsewhere (e.g., Nakamura, 1997; El Hilali et al., 2023), a comprehensive seismic microzonation framework for Malang has not yet been established. Therefore, this study aims to characterize the spatial variability of local site effects in Malang City by integrating single-station HVSR analysis from 19 microtremor measurement sites with geological and morphological information to identify zones with higher potential for ground-motion amplification and soil-related seismic vulnerability, within the limitations of ambient-noise data and spatial interpolation.

Malang features a complex geological setting from the combined influence of tectonic and volcanic processes. This region is situated in the southern part of the Kendeng Basin, which forms an integral segment of the East Java volcanic system. The geological evolution of this basin is strongly controlled by the ongoing convergence between the Indo-Australian Plate and the Eurasian Plate, a process that has driven intense subduction-related magmatism and crustal deformation. As a consequence, Malang is underlain by a thick sequence of young volcanic products, including lava flows, pyroclastic materials, and widespread Quaternary alluvial deposits, which were predominantly formed through endogenic geological activity associated with volcanic eruptions and tectonic uplift.

Geographically, Malang occupies a transitional zone between the northern and southern mountainous structures of Java Island, which significantly contributes to its diverse geomorphological characteristics. This transitional setting produces a wide range of landforms, from relatively flat alluvial plains to undulating volcanic slopes and dissected highlands. Such morphological diversity is accompanied by heterogeneous lithological compositions, reflecting variations in depositional environments, eruption styles, and subsequent erosion and sedimentation processes. The presence of heterogeneous and unconsolidated surface materials, particularly volcanic ash and alluvium, plays a crucial role in controlling local ground response to seismic waves, thereby increasing the spatial variability of seismic hazard across the Malang Area.

The city of Malang is located in the Solo–Gunungapi Quaternary Formation, which was formed during the Late Pleistocene to Holocene periods and is dominated by volcanic pyroclastic and epiclastic deposits, such as tuff, volcanic breccia, agglomerate, lava, and tuffaceous sand (El Hafidz Fatahillah et al., 2023). Regionally, this formation lies between the Kendeng Formation in the north and the Southern Mountains Formation in the south, with the

main geological units comprising lower Quaternary volcanic rocks (Qp), the Welang Formation (Qpw), Malang Tuff (Qvtm1), Arjuno –Welirang (Qvaw), and Kawi–Butak (Qpkb) volcanic rocks. Approximately 90% of the Malang City area is dominated by Tuf Malang, which originates from medium-composition volcanic pyroclastic deposits (Arif Kurnianto et al., 2019; Widya Saputra & Azmi, 2024).

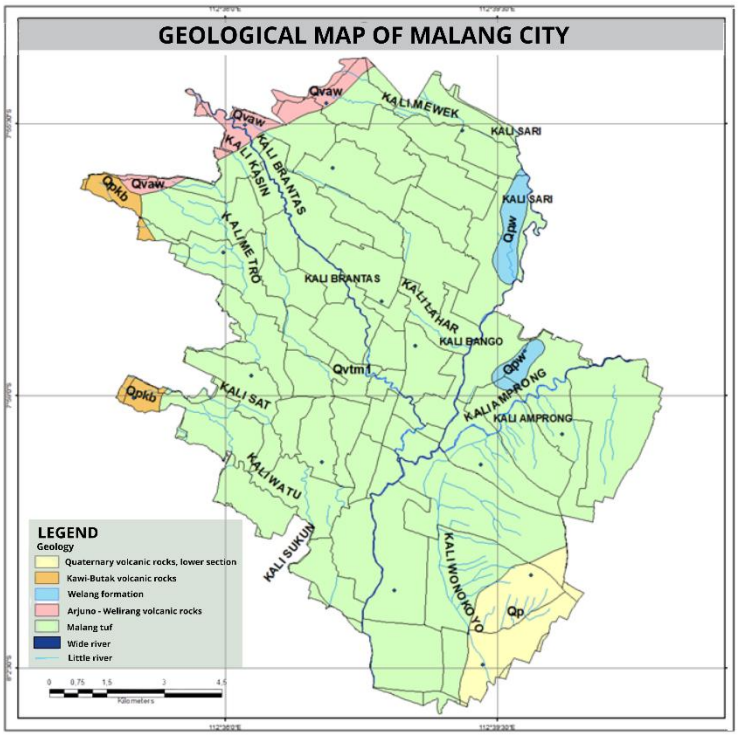

Figure 1. Geological Map of Malang City

This lithological heterogeneity results in significant seismic impedance contrasts, which directly affect the natural frequency (f_0) and amplification factor (A_0) identified through HVSR analysis (Huang et al., 2021; Araque-Perez, 2024). Young alluvial deposits (Qa) and fine tuffs, including the Mandalika Formation, generally have low shear wave velocities (Vs < ±300 m/s) and large thicknesses of soft sediments, thus being associated with low f_0 values (<2–3 Hz) and high amplification due to seismic wave trapping above deeper bedrock (Araque-Perez, 2024; Huang et al., 2021). Conversely, areas dominated by andesite breccia, lava, and compacted volcanic rocks have higher Vs (> 500–700 m/s) and thinner sediment thickness, resulting in higher f_0 and lower amplification.

The spatial distribution of extensive lowland alluvial units and more rigid volcanic units causes significant variations in HVSR response between regions in Malang City. In addition, morphological conditions such as steep slopes, high weathering rates, and the presence of water-saturated loose sediments reinforce local seismic responses, which have implications for landslide susceptibility and liquefaction potential during strong earthquakes (Bachri et al., 2021; Xue & Yang, 2016).

METHOD

Data Collection and Instrumentation

Based on the flowchart in Figure 2, the research process began with determining the microtremor recording points, which were set based on spatial distribution, accessibility, and surface conditions to ensure data acquisition quality. Measurements were taken using the East Java Regional Disaster Management Agency's Velbox SeismoWin device, which is capable of recording three components of ground vibration—vertical (Z) and horizontal N–S and E–W.

Each point was recorded for 20–30 minutes to obtain a stable signal and minimize interference from human activity and traffic. Sensors were placed on flat and stable ground to ensure accurate horizontal component orientation.

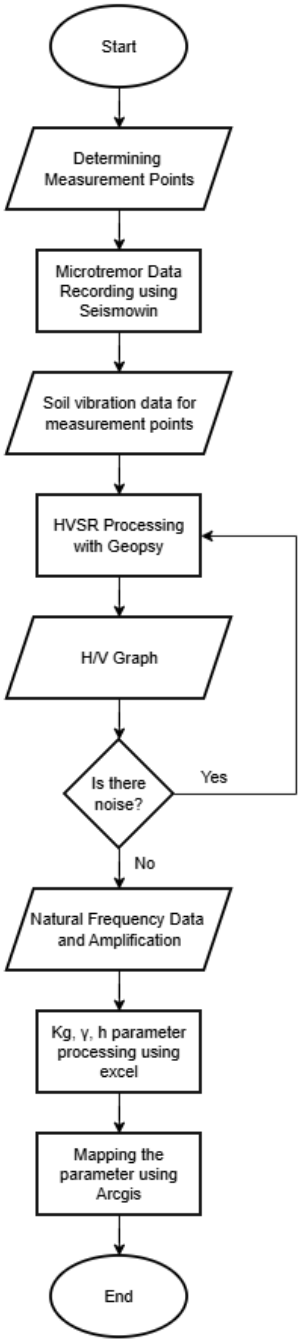

Figure 2. Data Processing Flowchart

The acquisition process was carried out over three days, from 09:00 to 19:00 WIB, under varying weather conditions from sunny to drizzly, with some locations in areas of heavy traffic. The selection of the measurement time and conditions was done to minimize anthropogenic noise, as recommended by Yulianto and Yuliyanto (2023). The microtremor data obtained was then processed using the HVSR method, which produced an H/V curve for each measurement point. From these curves, the natural frequency (f_0) was determined as the HVSR peak and the amplification factor (A_0) as the amplitude value at that peak. Based on f_0 and A_0, the derivative parameters Ag, Kg, and γ were then calculated, which were subsequently used in the mapping and spatial analysis process.

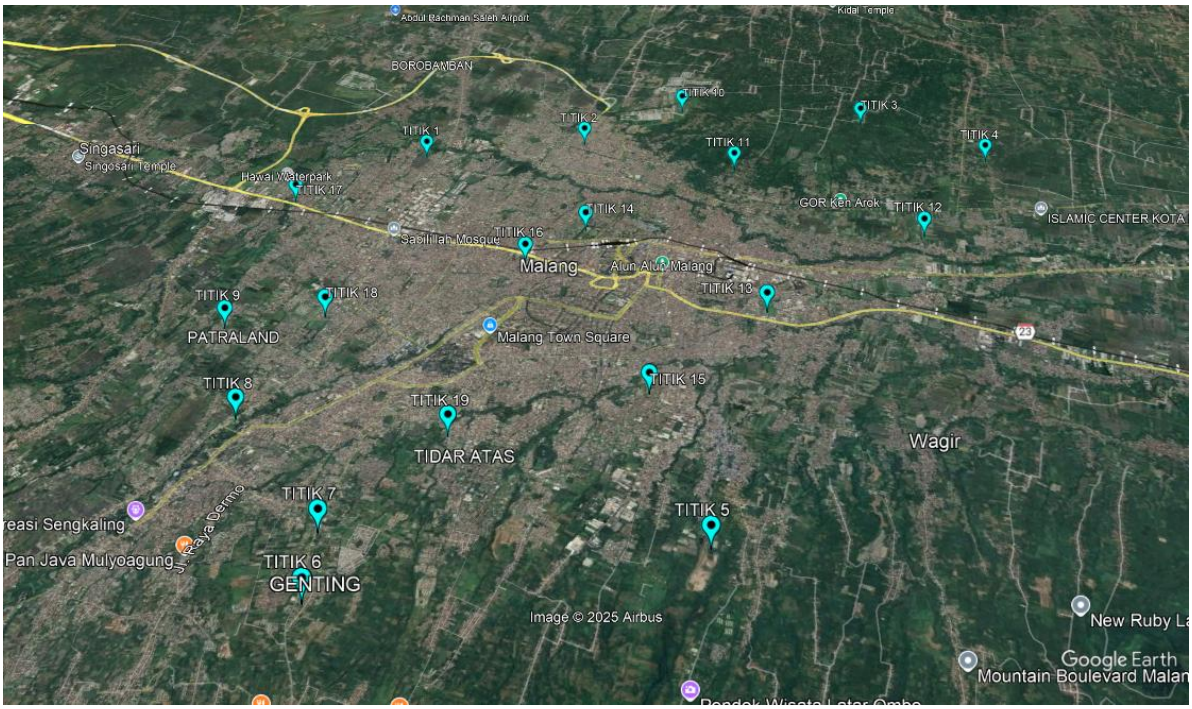

Figure 3. 19 Data Collection Points in Malang City

The study was conducted at 19 points in Malang City, East Java with geological complexity and significant variations in morphology and land use. The points were scattered in various areas, from the city center to areas that have hilly geological conditions and suburban areas. The point selection considers the geology of Malang City with elevation differences, building density, and subsurface impedance contrast (Cipta et al. 2024). Not only that, it also considers the access to the measurement area and the estimated time used. The point is depicted in Figure 3.

Table 1. Coordinates of Microtremor Measurement Points in Malang City

Point	Longitude	Latitude	District
Malang 1	112.66196	-7.94689	Blimbing
Malang 2	112.66424	-7.97377	Kedungkandang
Malang 3	112.66556	-8.02194	Kedungkandang
Malang 4	112.65517	-8.04104	Kedungkandang
Malang 5	112.58034	-7.98381	Sukun
Malang 6	112.57551	-7.93776	Lowokwaru
Malang 7	112.58516	-7.93824	Lowokwaru
Malang 8	112.60419	-7.92529	Lowokwaru
Malang 9	112.62163	-7.92067	Lowokwaru
Malang 10	112.67220	-7.99157	Kedungkandang
Malang 11	112.65480	-7.99820	Kedungkandang
Malang 12	112.63625	-8.02519	Kedungkandang
Malang 13	112.62067	-7.99768	Sukun
Malang 14	112.64078	-7.97264	Blimbing
Malang 15	112.60562	-7.97915	Sukun
Malang 16	112.63348	-7.96310	Lowokwaru
Malang 17	112.65088	-7.92649	Blimbing
Malang 18	112.62309	-7.93450	Lowokwaru
Malang 19	112.59967	-7.95273	Sukun

Based on the measurement coordinates shown in Table 1 and their distribution in Figure 3, microtremor points are scattered across five main subdistricts in Malang City, namely

Blimbing, Kedungkandang, Sukun, Lowokwaru, and Klojen. Most of the points are located in Kedungkandang and Lowokwaru, which represent areas with contrasting elevation and volcanic lithology, while the points in Sukun and Blimbing represent densely populated residential areas and areas with potential changes in subsurface impedance. This distribution ensures that diverse geological and morphological conditions are represented, so that the HVSR response obtained describes the variations in subsurface structure more comprehensively throughout the study area.

The measurement data were analyzed using the HVSR method proposed by Nakamura (1989) and refined by Konno and Ohmachi (1998). This method calculates the ratio of horizonal and vertical spectrum ratio to determine the natural frequency (F0) as an indicator of subsurface impedance. This method does not require an active wave source and can be applied simply (Molnar et al. 2022). The HVSR approach can be written as the following equation:

$$HVSR = \frac{\left[H_{NS}^2 + H_{WE}^2\right]^{1/2}}{V_S} \quad \text{…(eq 1)}$$

Additional validation was performed using Geopsy software by filtering noise to obtain an H/V curve. The filtering was performed using a smoothing process based on Konno-Ohmachi smoothing with a bandwidth of 40, a cosine type of 10%, and a window width of 20.00 s to ensure reliability at a frequency of 0.5 Hz, as per the characteristics of the H/V curve (SESAME, 2004). The curve provides information on the natural frequency and resonance potential of the site and minimizes the thickness of the sedimentary layer which can be used to evaluate the level of seismic susceptibility in the area(Lasmi Manginsih et al. 2023). In this study, the number of windowing used is at least 10 for each measurement point to ensure the stability of the HVSR curve [20]. Meanwhile, the smoothing process in spectrum analysis refers to the method of Konno dan Ohmachi, (1998), the better the quality of the waveform recordings obtained, the greater the number of windows that can be selected, so that the spectral analysis results become more accurate and more representative of the soil characteristics at the study site.

Kg dan *Y* Parameters

Deformation or shear strain of soil (Y) on a soil surface can be estimated based on the following equation:

$$\Upsilon = A_g \times \frac{\delta}{h} \quad \text{…(eq 2)}$$

Where A_g indicates the amplification factor, h indicates the sediment, and δ represents the seismic displacement from underground. If the velocity of the S wave underground and on the surface is denoted by Cb and Cs, then the natural frequency can be written in the following equation:

$$f_0 = \frac{C_b}{4A_g\, x\, h} \quad \text{…(eq 3)}$$

Acceleration underground can be written as the equation:

$$a_b = (2\pi f_0)^2 \times \delta \quad \text{…(eq 4)}$$

Substituting equations 2-4 will result in the following equation:

$$\Upsilon = \frac{A_g^2}{f_0} \times \frac{a_b}{\pi^2 C_b} \quad \text{…(eq 5)}$$

Assuming the efficiency of seismic force to static force is e%, then the effective Υ_e

$$\Upsilon_e = K_g(e) \times a_b \quad \text{…(eq 6)}$$

Where

$$K_g(e) = e \times \frac{\frac{\frac{A_g^2}{f_0}}{a_b}}{\frac{\pi^2 C_b}{100}} \quad \text{…(eq 7)}$$

The value of C_b estimated to be nearly constant over a wide area. If C_b is assumed to be 600 m/s, then $1/(\pi^2 \times C_b = 1.69 \times 10^{-6}$ (s/cm) is obtained, and if e = 60%, maka $K_g(e)$ according to Nakamura, 2009 is:

$$K_g = \frac{A_g^2}{\mathrm{F_0}} \quad \text{…(eq 8)}$$

Spatial Interpolation and Classification

The spatial analysis of these parameters was performed using the Ordinary Kriging method in GIS. This method estimates values at unmeasured locations using a weighted linear combination of nearby observation points and assumes that the data variability is stationary (D'Alessandro et al., 2014; Goovaerts, 1997). Modeling was performed using an experimental semivariogram and spherical model type in the kriging menu in ArcGIS based on goodness of fit criteria to accurately represent the spatial continuity of subsurface geology (Setianto & Triandini, 2013; Trevisani et al., 2017). A grid size of 50 meters was used to provide spatial detail on the density of measurement points and avoid excessive smoothing artifacts (Cipta et al., 2018).

RESULTS AND DISCUSSION

The windowing applied to the three-component microtremor recordings, where only stable segments of the signal are selected for HVSR analysis (figure 4). This step is critical for suppressing transient noise and improving the reliability of spectral estimates (Bonnefoy-Claudet et al., 2006; SESAME, 2004). Variations in signal amplitude across measurement points reflect differences in local geological conditions, with higher amplitudes generally associated with softer sediments and greater susceptibility to amplification. After window selection, the resulting H/V spectra provide robust estimates of the site's natural frequency, where most locations in Malang exhibit f_0 values of 2–4 Hz, indicating intermediate sediment thickness with moderate amplification potential. Low frequencies (< 1 Hz) and high-frequency peaks (> 5 Hz) were interpreted cautiously due to possible noise contamination and shallow bedrock effects (Nakamura, 1989). Overall, the windowing results support the spatial variability of site response and form the basis for the quantitative parameters summarized in Table 2.

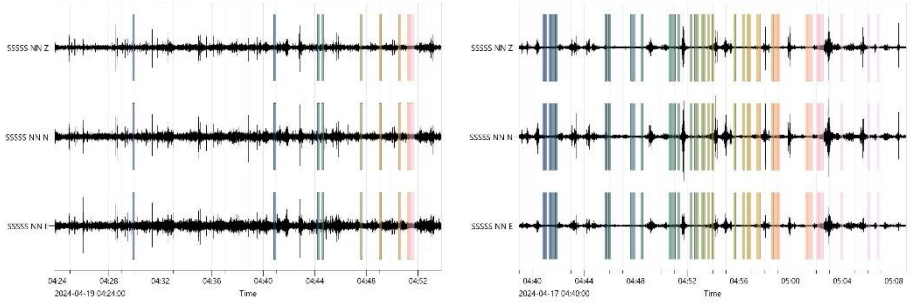

(a) (b)

Figure 1. Signal Graph Results of Malang 2 (a) and Malang 5 (b)

Based on the data presented in Table 2, the HVSR-derived parameters across Malang City exhibit substantial spatial variability, reflecting differences in local site response and soil dynamic characteristics. Among all measurement points, Malang 2 and Malang 5 stand out as the most seismically vulnerable sites due to the combined influence of low to moderate

fundamental frequency, high amplification, and elevated soil susceptibility index (Kg). At Malang 2, the fundamental frequency of 2.962 Hz is accompanied by the highest amplification factor (Ag = 6.639) and the maximum Kg value (14.871), together with a shear strain value (γ = 0.00922) that exceeds commonly accepted thresholds for nonlinear soil behavior, indicating a strong impedance contrast between sedimentary layers and underlying bedrock and a high potential for seismic resonance (Nakamura, 2000; Gosar, 2012). Similarly, Malang 5 is characterized by an even lower fundamental frequency of 1.413 Hz, a relatively high amplification factor of 4.496, and a Kg value of 14.306, as well as a large estimated sediment thickness (h = 23.612), suggesting deeper and more heterogeneous soil conditions that are prone to amplifying seismic vibrations, particularly for low- to medium-rise structures (SESAME, 2004; Bard, 2008).

Table 1. Data Processing Results at Measurement Points

Point	f_0	Ag	Kg	*Y*	h
Malang 1	4.400	6.099	8.454	0.00524	5.590
Malang 2	2.962	6.639	14.871	0.00922	7.623
Malang 3	2.433	4.535	8.453	0.00524	13.599
Malang 4	2.892	4.836	8.0934	0.00502	10.724
Malang 5	1.413	4.496	14.306	0.00887	23.612
Malang 6	3.038	4.595	6.949	0.00431	10.746
Malang 7	3.701	4.002	4.326	0.00268	10.127
Malang 8	9.938	2.685	0.726	0.00045	5.620
Malang 9	1.809	3.695	7.548	0.00468	22.444
Malang 10	3.437	5.137	7.677	0.00476	8.496
Malang 11	4.400	5.157	6.044	0.00375	6.611
Malang 12	2.493	4.893	9.600	0.00595	12.296
Malang 13	7.575	1.704	0.383	0.00024	11.624
Malang 14	1.809	4.073	9.173	0.00569	20.360
Malang 15	1.680	3.519	7.372	0.00457	25.381
Malang 16	1.809	3.877	8.312	0.00515	21.389
Malang 17	2.045	4.081	8.138	0.00505	17.962
Malang 18	1.448	3.424	8.093	0.00501	30.252
Malang 19	2.493	3.877	6.027	0.00374	15.519

In contrast, Malang 8 displays markedly different site response characteristics indicative of more stable subsurface conditions. This site exhibits a very high fundamental frequency of 9.938 Hz combined with a low amplification factor (Ag = 2.685), a minimal soil susceptibility index (Kg = 0.726), and a very low shear strain value (γ = 0.00045), all of which suggest shallow or highly compacted sediment overlying hard bedrock, thereby limiting resonance effects and reducing the potential for significant ground-motion amplification (D'Alessandro et al., 2016; Gosar, 2017). The pronounced contrast between the high-vulnerability signatures observed at Malang 2 and Malang 5 and the low-vulnerability response at Malang 8 highlights the effectiveness of HVSR parameters in discriminating subsurface conditions and seismic risk levels, which are further illustrated by the shape, sharpness, and peak frequency of the HVSR curves shown in Figure 5, graph of frequency against H/V at Malang 2, Malang 5, and Malang 8.

Figure 5 shows the HVSR graphs of Malang 2, Malang 5, and Malang 8 where there are significant variations in the natural frequency (f_0) and H/V amplification and illustrates the subsurface conditions and local seismic vulnerability. Malang 2 area shows a natural frequency of 2.9 Hz with an amplification of up to 6. The peak of the curve is sharp and symmetrical indicating an impedance contrast between the sedimentary and bedrock layers. This triggers site resonance in low- to medium-rise buildings (Nakamura, 2000; Gosar, 2012). These areas are found in urban areas. In another area, Malang area 5 shows a lower natural frequency of

1.4 Hz with an amplification of 4.5. This indicates deeper and heterogeneous soil characteristics that can amplify seismic vibrations (SESAME, 2004). In contrast, at Malang 8, the natural frequency value was very high at 9,938 Hz with a low amplification factor of 2,685. This indicates that the sediment layer at that point was shallow or very dense with hard bedrock. (D'Alessandro et al., 2016).

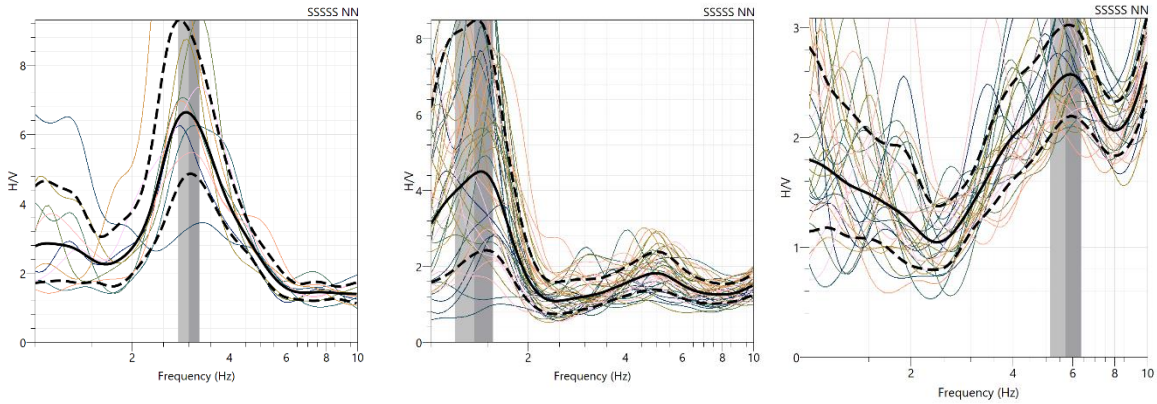

Figure 2. Graph of Frequency against H/V at Malang 2, Malang 5, and Malang 8

Natural Frequency Microzonation Map of Malang City

In figure 6, the lowest natural frequencies range from 0 Hz to 2 Hz in the western part of Sukun Subdistrict and the southern part of Klojen district. According to the soil classification by Nogoshi and Igarashi in 1970, the area is a sedimentary area or soft sediment. Based on the classification of Nogoshi dan Igarashi (1971), the natural frequency value of 0 - 2 Hz is included in the lowest group. This frequency can produce an amplification factor of 3 to 5 times (Pornsopin et al. 2024). The lower the natural frequency value, the more dangerous the soil. This is because in sediment layers with deep bedrock (trapped soft soil), it is able to trap seismic waves longer, causing a decrease in natural frequency and an increase in amplification (Roy et al 2020).

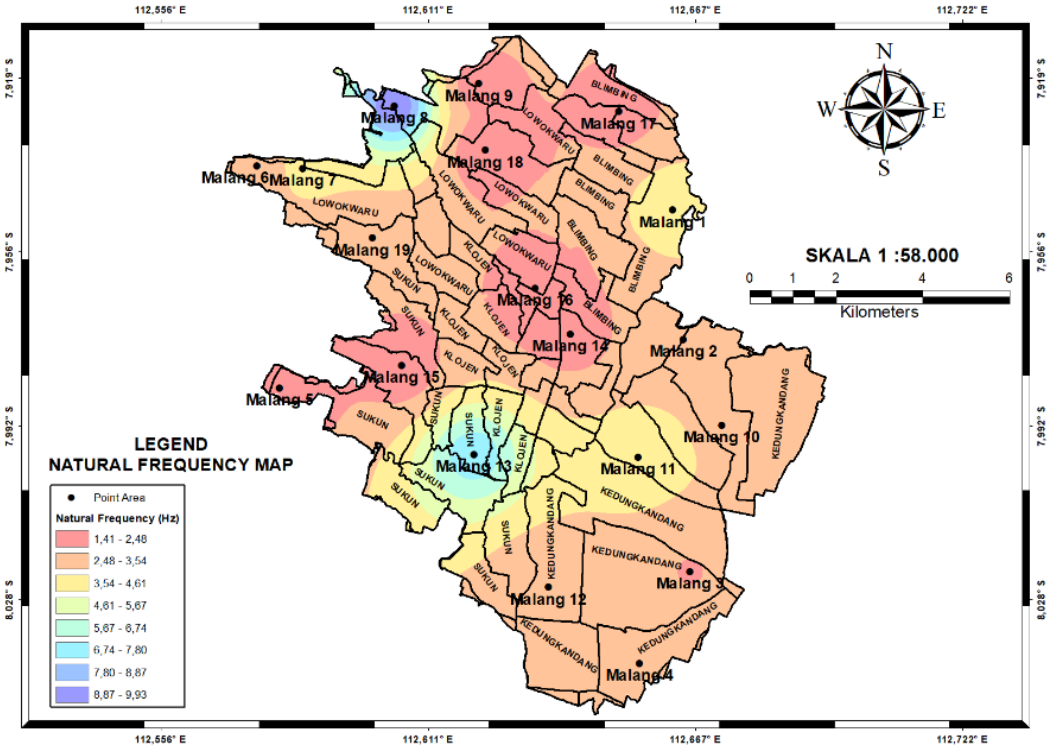

Figure 3. Natural Frequency Microzonation Map of Malang City

Moreover, the low natural frequencies and high amplification observed at Malang 2 and Malang 5 are consistent with the dynamic behavior of thick, weathered volcanic tuff layers that act mechanically as soft sediment despite being mapped as Malang Tuff (Qvtm1) and Kawi–Butak volcanic rocks (Qpkb). In such conditions, the contrast in shear-wave velocity between the soft volcanic cover and the underlying stiffer units can reproduce the same resonance pattern as deep sedimentary basins, thereby justifying the classification of these zones as seismically vulnerable soft-soil sites.

Table 3 summarizes the spatial distribution of natural frequency classes across districts, revealing marked contrasts in areal dominance that reflect variations in subsurface stiffness and sediment thickness. Districts such as Lowokwaru, Sukun, and Klojen exhibit substantial areal coverage across multiple frequency classes, indicating heterogeneous soil conditions with alternating zones of soft to moderately stiff sediments, which are commonly associated with complex site-response behavior. In particular, Sukun shows consistently large areas in intermediate to higher frequency classes, suggesting widespread variability in near-surface materials, while Lowokwaru displays the broadest distribution across all eight classes, implying strong lateral changes in soil properties. By contrast, districts such as Pakishaji, Tajinan, Tumpang, Pakis, and Singosari are characterized by limited representation in only a few frequency classes, reflecting more uniform subsurface conditions or smaller extents of soft sediment deposits. The total area statistics indicate that Classes 3, 4, and 5 dominate the study area, highlighting the prevalence of low- to medium-frequency site conditions that are typically associated with thicker sedimentary layers and an increased potential for seismic wave amplification, as widely recognized in HVSR-based microzonation studies (Nakamura, 2008; Bard, 2008).

Table 2. Area District of Natural Frequency Parameter

District	Area (m^2)							
	Class 1	**Class 2**	**Class 3**	**Class 4**	**Class 5**	**Class 6**	**Class 7**	**Class 8**
Pakishaji	-	-	-	67404.98	85788.16	-	-	-
Wagir	140937.69	159320.87	3063.86	-	21447.04	24510.90	-	-
Kedung Kandang	-	251236.76	5349504.65	13597423.61	14115216.4	5484314.61	134809.97	-
Tajinan	-	-	-	499409.65	-	-	-	-
Tumpang	-	-	104171.34	3063.863	-	-	-	-
Lowokwaru	2451090.33	5064565.40	5018607.45	2699263.23	3140459.49	1320524.92	781285.04	658730.53
Karangploso	39830.22	116426.79	85788.16	12255.45	15319.31	24510.90	70468.85	24510.90
Dau	-	67404.98	33702.49	217534.27	315577.88	30638.63	24510.90	88852.02
Sukun	1954744.54	2187598.12	4004468.83	1927169.77	2132448.59	3112884.72	2448026.47	1605464.17
Klojen	1145884.73	1617719.62	2668624.60	1296014.01	805795.95	707752.33	1053968.84	499409.65
Pakis	-	-	-	45957.94	33702.49	-	-	-
Blimbing	1277630.84	4580475.05	4353749.20	3174161.98	2687007.77	1611591.89	-	-
Singosari	-	82724.299	422813.08	3063.86	-	-	-	-
Area Total	539239.87	1086728.61	1695730.28	1810978.66	1796366.39	947440.69	347159.24	221305.18

Amplification Microzonation Map of Malang City

The soil amplification value represents the change in ground motion acceleration from bedrock to surface (Partono. et al. 2023). Amplification can also be interpreted as how much the soil can amplify earthquake waves (Sedaghati et al. 2018). Figure 7 shows that the soil amplification of Malang City ranges from 1.72 - 6.63. The smallest amplification results, namely amplification below <3, are located in the western and southern parts of Malang City, such as in the western Lowokwaru District and the southern Kedungkandung District. This low value indicates that the soil characteristics are dominated by hard and dense bedrock, such as old volcanic rocks, breccias, and sedimentary rock formations that have undergone complete lithification. This condition causes seismic waves that propagate through these layers to not

experience significant strengthening or amplification or in other words, no amplification occurs.

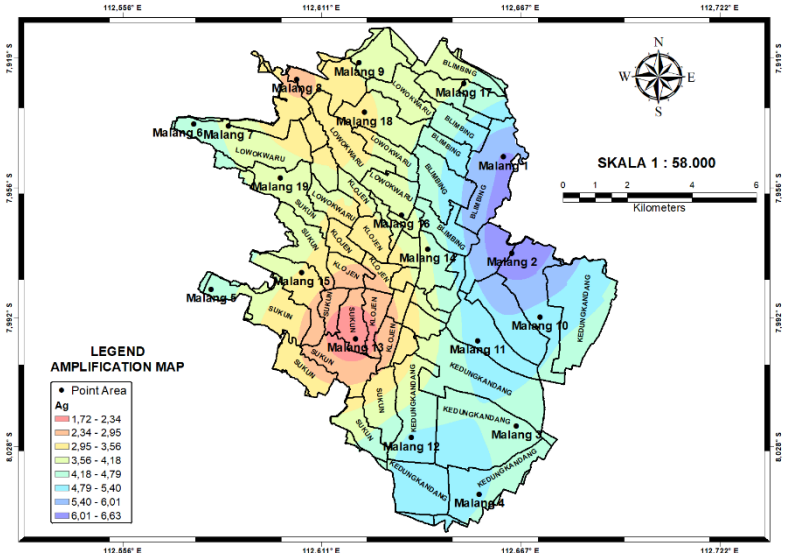

Figure 4. Amplification Microzonation Map of Malang City

High amplification with a value of (5.4 - 6.63) was identified in the eastern part of Malang City, especially in most areas of Kedungkandang district and the eastern part of Blimbing district. It shows loose sedimentary material derived from fluval sedimentation and young volcanics. The constituent materials are sand, clay, gravel and volcanic ash that have low density and minimal cohesion, causing high amplification. The thickness of the sedimentary layer in this area is large enough to trap the energy of seismic waves coming from the subsurface. This condition causes seismic wave energy to be trapped and amplified as it propagates through the ground, increasing the potential for damage during an earthquake (Pornsopin et al. 2024; Stanko et al. 2017).

Table 3. Area District of Amplification Parameter

District	Area (M^2)							
	Class 1	Class 2	Class 3	Class 4	Class 5	Class 6	Class 7	Class 8
Pakishaji	-	-	-	85788.16	33702.49	33702.49	-	-
Wagir	-	33702.49	33702.49	153193.15	128682.24	-	-	-
Kedung Kandang	-	606644.86	1246992.21	1703507.78	6814031.12	19443274.04	5530272.56	3587783.47
Tajinan	-	-	-	-	3676.35	4626.30	-	-
Tumpang	-	-	-	-	107235.20	-	-	-
Lowokwaru	21447.04	3780806.83	10123003.06	6881436.10	1170395.63	-	-	-
Karangploso	-	128682.24	137873.83	131746.11	-	-	-	-
Dau	-	88852.02	55149.53	349280.372	284939.25	-	-	-
Sukun	4166853.56	4798009.32	4647880.04	4372132.38	1375674.45	12255.45	-	-
Klojen	1645294.38	3826764.78	3645996.87	640347.35	36766.35	-	-	-
Pakis	-	-	-	-	-	18383.18	9191.59	52085.67
Blimbing	-	-	254300.62	3725657.30	4779626.14	3403951.70	3198672.89	2322408.09
Singosari	-	-	-	407493.77	98043.61	3063.86	-	-
Area Total	448738.08	1020266.35	1549607.59	1419275.57	1143527.91	1798251.85	672164.39	458636.71

The spatial distribution of seismic amplification across districts reveals pronounced variability in site-response characteristics, reflecting differences in near-surface soil stiffness and sediment thickness, as summarized in Table 4. Districts such as Kedung Kandang, Lowokwaru, Sukun, Klojen, and Blimbing dominate the higher amplification classes, indicating the presence of soil conditions that are more susceptible to ground-motion amplification. In particular, Kedung Kandang exhibits the largest areal extent within Classes 5 to 8, with especially extensive coverage in Class 6 and Class 7, which suggests thick, laterally heterogeneous sedimentary deposits capable of significantly amplifying seismic waves.

Lowokwaru and Sukun also show broad distributions across intermediate to high amplification classes, implying complex subsurface conditions and variable soil stiffness in densely urbanized areas. In contrast, districts such as Pakishaji, Tajinan, Tumpang, Pakis, and Singosari are characterized by limited areal coverage and confinement to lower or intermediate amplification classes, reflecting relatively more stable subsurface conditions or smaller extents of amplification-prone soils. Overall, the dominance of Classes 4 to 6 in the total area highlights the prevalence of moderate to high amplification potential across the region, a pattern that is consistent with HVSR-based evaluations of seismic site effects in sedimentary and urban environments (Nakamura, 2008; Bard, 2008).

Soil Vulnerability Index Microzonation Map of Malang City

Figure 8 shows the distribution of the soil vulnerability index in Malang City. Based on the figure, there are several classifications or classes of soil susceptibility index values. The lowest soil susceptibility index in Malang City is 2.45 - 3.7 in Karang Ploso and Sukun areas. The dominating soil susceptibility index value in Malang City is 7.8 - 8.9 with locations in Blimbing, Klojen, Lowokwaru, Kedung Kandang, Tumpang, Pakis, and Singosari. However, two extreme points, Malang 2 in the north of Kedungkandang and Malang 5 in the west of Sukun, have soil susceptibility of 14.87 and 14.30. This parameter combines the two main parameters of HVSR, namely amplification and natural frequency. One of the North Morocco microzonation studies mentioned that areas with Kg>10 values with Quaternary sedimentary layers have a high risk of liquefaction and resonance (EL Hilali et al. 2023).

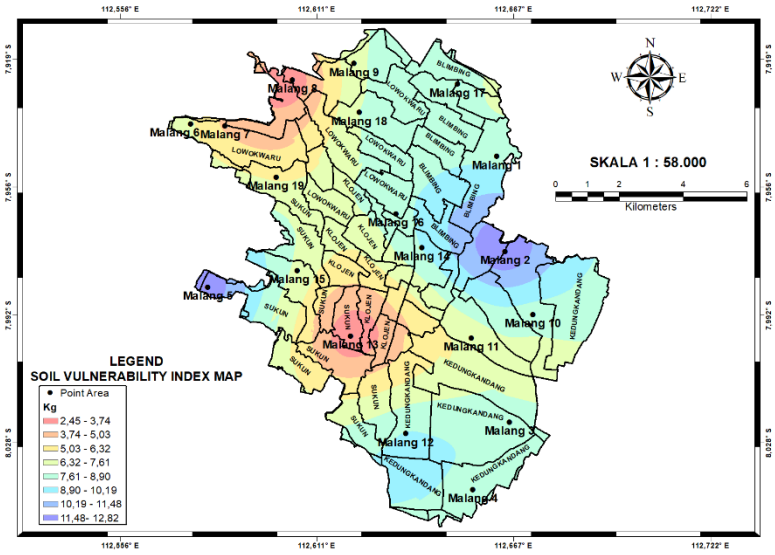

Figure 5. Soil Vulnerability Index Microzonation Map of Malang City

Furthermore, through calculations assuming (γ) >10^{-2} here the soil conditions have the potential for liquefaction by determining the Kg threshold value which causes the soil shear-strain magnitude (γ) >10-2. By assuming based on Nakamura (1997), wave velocity and acceleration of bedrock vibrations with a Vb value of 600 m/s and ab value according to research by Kumala dan Wahyudi (2016), amounting to 0,375 g or 367,5 gal, soil shear-strain magnitude (γ) 0,3 - 0,9.

Table 4. Area District of Soil Vulnerability Parameter

District	Area (m2)							
	Class 1	**Class** 2	**Class** 3	**Class** 4	**Class** 5	**Class** 6	**Class**7	**Class** 8
Pakishaji	-	-	-	18383.18	79660.44	55149.53	-	-
Wagir	-	-	30638.63	15319.31	9191.59	101107.48	58213.40	134809.97
Kedung Kandang	24510.90	1905722.73	3505059.17	8974054.47	10460027.98	9185461.01	2371429.89	2506239.86
Tajinan	-	-	-	-	235917.44	263492.21	-	-

District	Area (m2)							
	Class 1	**Class** 2	**Class** 3	**Class** 4	**Class** 5	**Class** 6	**Class**7	**Class** 8
Tumpang	-	-	-	6127.73	101107.48	-	-	-
Lowokwaru	2236619.93	4522261.66	3713401.86	4748987.51	6627135.48	128682.24	-	-
Karangploso	18383.18	122554.52	85788.16	171576.32	-	-	-	-
Dau	1317411	49021.81	459579.44	82724.30	49021.81	6127.73	-	-
Sukun	2466409.65	3345738.30	5089076.30	4773498.41	1905722.73	937542.05	284939.25	569878.50
Klojen	1544186.91	173414 6.41	24051 32.39	2864711.82	1017202.49	229789.72	-	-
Pakis	-	-	-	-	-	18383.18	21447.04	39830.22
Blimbing	-	-	597453.27	1896531.14	7570805.25	4344557.61	3069990.64	205278.82
Singosari	-	-	-	101107.48	407493.77	-	-	-
Area Total	493988.97	898418.88	1222009.94	1819463.21	2189483.57	1174637.90	446616.94	265849.03

The Ground shear-strain parameter is related to soil damage in that it is directly proportional to the soil damage that can occur. A stretched soil is characterized quite easily by building damage. Some of the phenomena caused by stretching are cracks, subsidence, landslides, and even liquefaction. Landslides and liquefaction occur when $(\gamma) > 10^{-2}$ [Rasouli, Towhata, and Hayashida 2015; Nakamura. 1997). Figure 8 shows that in this study, high soil shear-strain values are located in Malang 2 and Malang 5.

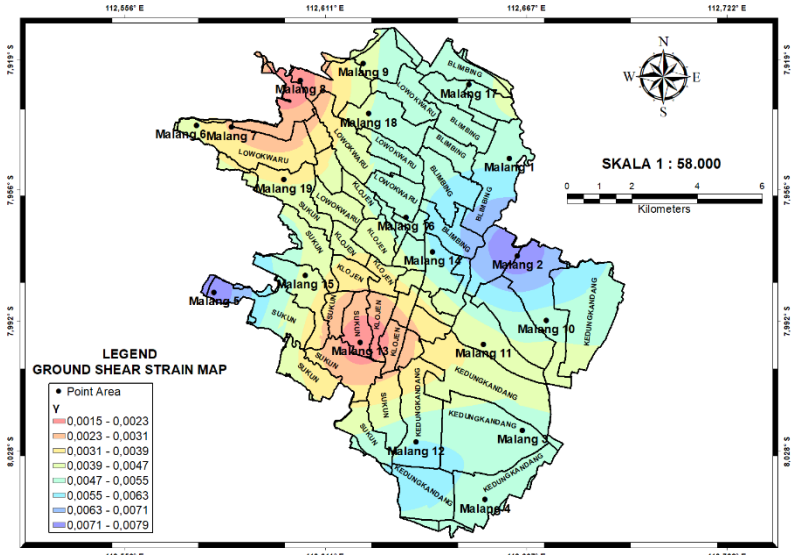

Figure 6. Ground Shear-Strain Microzonation Map of Malang City

The spatial distribution of ground shear-strain in Malang City shows a clear heterogeneity that reflects variations in subsurface geological conditions and local seismic response, as illustrated in Figure 9. Areas characterized by low shear-strain values (represented by cooler colors) indicate relatively stiff or shallow subsurface layers that are less susceptible to deformation during seismic shaking, whereas zones with moderate to high shear-strain values (warmer colors) correspond to thicker and softer sedimentary deposits that tend to amplify ground deformation. Higher shear-strain classes are predominantly observed in the central to southern parts of the city, implying a greater potential for ground deformation and structural damage during earthquake events, while the outer districts generally exhibit lower strain levels. This spatial pattern emphasizes the relevance of ground shear-strain microzonation in seismic risk assessment and urban development planning, which is subsequently supported by the areal statistics of each shear-strain class presented in Table 6.

Table 5. Area District of Ground Shear-Strain Parameter

District	Area (m^2)							
	Class 1	Class 2	Class 3	Class 4	Class 5	Class 6	Class7	Class 8
Pakishaji	-	-	-	18383.18	79660.44	55149.53	-	-
Wagir	-	-	30638.63	15319.31	9191.59	101107.48	58213.40	134809.97
Kedungkandang	24510.90	1905722.73	3505059.17	897404.47	10460027.98	9185461.01	2371429.89	2506239.86

District	Area (m^2)							
	Class 1	Class 2	Class 3	Class 4	Class 5	Class 6	Class7	Class 8
Tajinan	-	-	-	-	235917.44	263492.21	-	-
Tumpang	-	-	-	6127.73	101107.48	-	-	-
Lowokwaru	2236619.93	4522261.66	3713401.86	4748987.51	6627135.48	128682.24	-	-
Karangploso	18383.18	122554.52	85788.16	171576.32	-	-	-	-
Dau	131746.11	49021.81	459579.44	82724.30	49021.81	6127.73	-	-
Sukun	2466409.65	3345738.30	5089076.30	4773498.41	1905722.73	937542.05	284939.25	569878.50
Klojen	1544186.91	1734146.41	2405132.39	2864711.82	1017202.49	229789.72	-	-
Pakis	-	-	-	-	-	18383.18	21447.04	39830.22
Blimbing	-	-	597453.27	1896531.14	7570805.25	4344557.61	3069990.64	205278.82
Singosari	-	-	-	101107.48	407493.77	-	-	-
Area Total	493988.97	898418.88	1222009.94	1819463.21	2189483.57	1174637.90	446616.94	265849.03

The spatial distribution of ground shear-strain classes shows a clear dominance of moderate to high deformation potential across several districts, reflecting variations in subsurface stiffness and seismic response, as summarized in Table 6. Kedungkandang represents the most critical area, with very large extents in Classes 4, 5, and 6, indicating zones where seismic shaking is likely to induce significant shear deformation due to soft and thick sedimentary layers. Sukun and Blimbing also exhibit extensive coverage in intermediate to high classes, particularly Classes 3–6, suggesting widespread susceptibility to strain accumulation under strong ground motion. In contrast, districts such as Pakishaji, Tumpang, Tajinan, and Singosari show more localized distributions, mainly confined to specific classes, implying relatively limited but still notable deformation-prone zones. Overall, the total area is largely concentrated in Classes 4 and 5, emphasizing that moderate ground shear-strain levels prevail across the study area, which is crucial for seismic microzonation and for assessing potential damage to structures sensitive to ground deformation.

Discussion

The results of this study address this research gap by demonstrating that the combined interpretation of HVSR parameters—natural frequency (f_0), amplification (Ag), soil susceptibility index (Kg), and ground shear-strain (γ)—provides a more comprehensive and spatially consistent assessment of seismic vulnerability in Malang City, where areas with low f_0 and high Ag and Kg systematically correspond to elevated shear-strain values, a relationship that has not been explicitly quantified in many previous urban-scale studies that relied on single-parameter analyses or sparse measurement points (Nakamura, 2000; SESAME, 2004; Gosar, 2012; D'Alessandro et al., 2016). Research conducted in the Yogyakarta Basin shows that an area with low frequency (< 1 Hz) and high vulnerability index should have a high priority level in disaster preparedness (Sunardi et al. 2025). Studies in Padalarang show that a natural frequency of 1.4-HZ with an amplification factor A0 of 2-8 has a susceptibility index ranging from 1-30, indicating moderate to high susceptibility (Januarta et al. 2020). The study in Pandang with a natural frequency of 0.5-1.9 Hz has an amplification value of 0.6 - 9.7 with an indication that the entire area has a high seismic potential (Susilanto et al. 2016). Not only that, studies in David City, Panama show natural frequency values ranging from 0.5-1.5 HZ with sediment thickness >50 m have high seismic vulnerability where it is composed of alluvial deposits (Grajales-Saavedra et al. 2023). Study in Wilga Basin, HVSR method can map the architecture of the main basin with deposits in the basin that are not well identified (Stannard et al. 2019).

CONCLUSION

Based on the results of HVSR analysis in Malang City, this study shows variations in dominant frequency characteristics, amplification factors, soil vulnerability indices, and ground shear strain that reflect heterogeneous geological conditions and sediment dynamics. The dominant frequency values, which are generally in the low to medium range, accompanied by significant amplification variations in several locations, indicate the presence of sediment

layers with varying thickness and compactness as well as a fairly strong impedance contrast between the surface layer and the bedrock. This pattern is consistent with the geological character of Malang, which is located in a volcanic-tectonic transition zone, but reveals spatial details of vulnerability that have not been widely reported in previous studies, which tended to focus on single parameters or limited measurement points.

The novelty of this study lies in the presentation of seismic microzonation based on the integration of several HVSR parameters—dominant frequency, amplification, soil vulnerability index, and ground shear strain—which are analyzed spatially to describe the level of local soil response more comprehensively. This approach expands on previous findings that generally emphasized only natural frequency and amplification, adding an interpretation of soil deformation relevant to potential building damage. However, this study still has limitations, particularly regarding the density of measurement points and the unavailability of supporting data such as geotechnical borehole data, Vs30, and actual ground motion records for quantitative validation. Therefore, further research is recommended to combine the HVSR method with more detailed subsurface data, increase the density of measurement stations, and perform validation using recorded earthquake data, so that the resulting microzonation map can further strengthen the basis for spatial planning and earthquake risk mitigation in Malang City.

RECOMMENDATION

Based on this study, it is recommended that further research integrate the HVSR method with other supporting data such as Vs30 and MASW or ReMi to quantitatively validate the parameters. These parameters are then integrated with building inventory data in terms of structure type, height, and building age to evaluate the potential for ground resonance on buildings in a practical manner for disaster mitigation and spatial planning.

ACKNOWLEDGMENTS

The author would like to express his deepest gratitude to the Regional Disaster Management Agency (BPBD) of East Java and all parties involved in this study for the support of facilities and knowledge that greatly assisted in the implementation of this research.

AUTHOR CONTRIBUTIONS STATEMENT

This study applies the Contributor Roles Taxonomy (CRediT) to describe the contributions of each author as follows:

Name of Author	C	M	So	Va	Fo	I	R	D	O	E	Vi	Su	P	Fu
Adedio Daniel Situmeang	✓	✓	✓	✓	✓	✓		✓	✓	✓			✓	
Yuansyah Dhaniar Ramadhan	✓	✓		✓		✓		✓	✓	✓		✓		
M. Rizky Saputra			✓	✓		✓	✓	✓	✓		✓		✓	
Divana Zumrotul Asyfiya							✓		✓			✓	✓	
Safira Nur Cholisatin							✓		✓			✓	✓	
Alif Haidar Safrian	✓		✓	✓	✓	✓		✓			✓	✓		
Rasamala I.W Putri						✓		✓			✓	✓	✓	
Madlazim		✓		✓	✓		✓		✓	✓		✓		
Arie Realita		✓		✓	✓		✓		✓	✓		✓	✓	
M. Nurul Fahmi		✓		✓	✓		✓		✓	✓		✓		

C : **C**onceptualization
M : **M**ethodology
So : **So**ftware
Va : **Va**lidation
Fo : **Fo**rmal analysis
I : **I**nvestigation
R : **R**esources
D : **D**ata Curation
O : Writing - **O**riginal Draft
E : Writing - Review & **E**diting
Vi : **Vi**sualization
Su : **Su**pervision
P : **P**roject administration
Fu : **Fu**nding acquisition

CONFLICT OF INTEREST STATEMENT

Authors state no conflict of interest.

INFORMED CONSENT (if applicable) (10 PT)
We have obtained informed consent from all individuals included in this study.

REFERENCES

Araque-Perez, C. J. (2024). Reevaluating Soil Amplification Using Multi-Spectral HVSR Technique In La Chana Neighborhood, Granada, Spain. *Journal of Seismology, 28*(4), 921–949.

Arif Kurnianto, F., Baskara, M. R. A., Alfani, A. F., & Lestari, N. (2019). An Overview Of Landscapes And Stratigraphy In Tertiary And Quaternary Volcanic Regions Of East Java, Indonesia. *International Journal of Scientific & Technology Research, 8*, 7.

Athanasius Cipta, Afif, H., Pradipto, M. J. A., et al. Optimizing HVSR Curves, Slope And Geologic Information For Vs30 And Seismic Vulnerability Zoning In Likupang. *Jurnal Lingkungan dan Bencana Geologi*.

Bachri, S., Shrestha, R. P., Yulianto, F., Sumarmi, Utomo, K. S. B., & Aldianto, Y. E. (2021). Mapping Landform And Landslide Susceptibility Using Remote Sensing, GIS And Field Observation In The Southern Cross Road, Malang Regency, East Java, Indonesia. *Geosciences, 11*(1), 1–15.

Bonnefoy-Claudet, S., Cotton, F., & Bard, P. Y. (2006). The Nature Of Noise Wavefield and Its Applications for Site Effects Studies: A literature review. *Earth-Science Reviews, 79*(3–4), 205–227.

D'Alessandro, A., Luzio, D., Martorana, R., & Presti, V. L. (2016). HVSR Analysis For Seismic Microzonation: New Constraints From Joint Inversion Of Rayleigh Wave Dispersion And H/V Spectral Ratios. *Soil Dynamics and Earthquake Egineering, 88*, 235–248.

El Hafidz Fatahillah, Hilmi, Ratna, P. N., Septiawan, F., Pratama, R. N., Al Ghiffari, M. R., Wicaksono, N., & Hidayat, W. Identifikasi Distribusi Formasi Breksi Volkanik Terkait Potensi Akuifer Air Tanah Menggunakan Pemodelan Resistivitas 3D. *Jurnal Lingkungan dan Bencana Geologi*.

EL Hilali, M., Bounab, A., Timoulali, Y., El Messari, J. E. S., & Ahniche, M. (2023). Seismic Site-Effects Assessment In A Fluvial Sedimentary Environment: Case Of Oued Martil Floodplain, Northern Morocco. *Natural Hazards, 118*(2).

Gosar, A. (2012). Site Effects And Soil–Structure Resonance Study In The Kobarid Basin (NW Slovenia) Using Microtremors. *Natural Hazards and Earth System Sciences, 12*(3), 761–772.

Gosar, A. (2017). Study On The Applicability Of The Microtremor HVSR Method To Support Seismic Microzonation In The Town Of Idrija (W Slovenia), 925–937.

Grajales-Saavedra, F., Mojica, A., Ho, C., Samudio, K., Mejía, G., Li, S., Almengor, L., Miranda, R., & Muñoz, M. (2023). Horizontal-To-Vertical Spectral Ratios And Refraction Microtremor Analyses For Seismic Site Effects And Soil Classification In The City Of David, Western Panama. *Geosciences, 13*(10).

Hernanti, H. Y., Kristiawan, S. A., & As'ad, S. (2009). Bangunan Rusunawa Lubuk Buaya Padang. Evaluasi Kerentanan Bangunan Rusunawa Lubuk Buaya Padang. *Jurnal Teknik Sipil*, 2(1), 1–8.

Huang, D., Wang, G., Du, C., & Jin, F. (2021). Seismic Amplification Of Soil Ground With Spatially Varying Shear Wave Velocity Using 2D Spectral Element Method. *Journal of Earthquake Engineering, 25*(14), 2834–2849.

Januarta, G. H., Yudistira, T., Tohari, A., & Fattah, E. I. (2020). Mikrozonasi Seismik Wilayah Padalarang Menggunakan Metode HVSR. *Riset Geologi dan Pertambangan, 30*(2), 143.

Konno, K., & Ohmachi, T. (1998). Ground-Motion Characteristics Estimated From Spectral Ratio Between Horizontal And Vertical Components Of Microtremor. *Bulletin of the Seismological Society of America, 88*(1).

Kumala, D., & Wahyudi, D. (2016). Evaluasi Tingkat Percepatan Maksimum Tanah Akibat Gempa Bumi Di Pulau Jawa. *Jurnal Teknik Sipil*, *23*(1), 23–32.

Lasmi Manginsih, S., Praja, N. K., et al. (2023). Soil Layer Mapping Using HVSR Microtremor Data And Its Impact On The Carrying Capacity Of Soil In Kendari City. *Jurnal Geologi dan Sumberdaya Mineral*, 24(1), 1–14.

Maklad, M., Yokoi, T., Hayashida, T., ElGabry, M. N., Hassan, H. M., Hussein, H. M., Fattah, T. A., & Rashed, M. (2020). Site Characterization In Ismailia, Egypt Using Seismic Ambient Vibration Array. *Engineering Geology*, *279*.

Molnar, S., Cassidy, J. F., Castellaro, S., Cornou, C., Crow, H., Hunter, J. A., Matsushima, S., Sánchez-Sesma, F. J., & Yong, A. (2018). Application Of MHVSR Analysis For Site Characterization: State Of The Art. *Surveys in Geophysics*, *39*(4), 613–631.

Molnar, S., Sirohey, A., Assaf, J., Bard, P. Y., Castellaro, S., Cornou, C., Cox, B., et al. (2022). A Review Of The Microtremor HVSR Method. *Journal of Seismology*, *26*(4), 653–685.

Mundepi, A. K., & Mahajan, A. K. (2010). Site Response Evolution And Sediment Mapping Using HVSR In Jammu City, NW India. *Journal of the Geological Society of India*.

Muttaqy, F., Nugraha, A. D., Mori, J., Puspito, N. T., & Supendi, P. (2022). Seismic Imaging Of Lithospheric Structure Beneath Central–East Java, Indonesia. *Frontiers in Earth Science*, *10*.

Muttaqy, F., Nugraha, A. D., Puspito, N. T., Sahara, D. P., Zulfakriza, Rohadi, S., & Supendi, P. (2023). Double-Difference Earthquake Relocation In Central And East Java, Indonesia. Geoscience Letters, 10(1).

Nagamani, D., Sivaram, K., Rao, N. P., & Satyanarayana, H. V. S. (2020). Ambient Noise And Earthquake HVSR Modelling For Site Characterization In Southern Mainland Gujarat. *Journal of Earth System Science*, *129*(1).

Nakamura, Y. (1989). A Method For Dynamic Characteristics Estimation Of Subsurface Using Microtremor On The Ground Surface. *Quarterly Report of RTRI*, *30*(1), 25–33.

Nakamura, Y. (1997). Seismic Vulnerability Indices For Ground And Structures Using Microtremor. World Congress On Railway Research, Florence, Italy.

Nakamura, Y. (2000). Clear Identification Of Fundamental Idea Of Nakamura's Technique And Its Applications. Proceedings Of The 12th World Conference On Earthquake Engineering, Auckland, New Zealand.

Nogoshi, M., & Igarashi, T. (1970). On The Propagation Characteristics Of Microtremors. Journal Of The Seismological Society Of Japan, *23*, 264–280.

Nogoshi, M., & Igarashi, T. (1971). On The Amplitude Characteristics Of Microtremor (Part 2). *Proceedings of the 17th JSCE Earthquake Engineering Symposium*, 26–40.

Partono, W., Irsyam, M., Prabandiyani, S. R. W., & Maarif, S. (2013). Aplikasi Metode HVSR Pada Perhitungan Faktor Amplifikasi Tanah Di Kota Semarang. *Media Komunikasi Teknik Sipil*, 19(2), 129–132.

Pornsopin, P., Pananont, P., Furlong, K. P., Chaila, S., Promsuk, C., Kamjudpai, C., & Phetkongsakul, K. (2024). Seismic Microzonation Map Of Chiang Mai Basin, Thailand. *Trends in Sciences*, *21*(3).

Rasouli, R., Towhata, I., & Hayashida, T. (2015). Mitigation Of Seismic Settlement Of Light Surface Structures By Installation Of Sheet-Pile Walls. *Soil Dynamics and Earthquake Engineering*, *72*, 108–118.

Ridwan, M., Cummins, P. R., Widiyantoro, S., & Irsyam, M. (2019). Site Characterization Using Microtremor Array And Seismic Hazard Assessment For Jakarta, Indonesia. In *Estimation of S-wave Velocity Structures by Using Microtremor Array* (pp. 1–10). Bandung: ITB Press.

Roy, N., Mukherjee, S., & Sahu, R. B. (2020). Influence Of Trapped Soft/Stiff Soil Layer In Seismic Site Response Analysis. *Journal of Earth System Science*, *129*(1).

Sedaghati, F., Pezeshk, S., & Nazemi, N. (2018). Site Amplification Within The Mississippi Embayment. *Soil Dynamics and Earthquake Engineering, 113*, 534–544.

SESAME European Research Project. (2004). Guidelines For The Implementation Of The H/V Spectral Ratio Technique On Ambient Vibrations. European Commission.

Stanko, D., Markušić, S., Strelec, S., & Gazdek, M. (2017). HVSR Analysis Of Seismic Site Effects And Soil–Structure Resonance In Varaždin City. *Soil Dynamics and Earthquake Engineering, 92*, 666–677.

Stannard, D., Meyers, J., & Dronfield, T. (2019). Passive Seismic Horizontal-To-Vertical Spectral Ratio (HVSR) Surveying To Help Define Bedrock Depth. *Exploration Geophysics*, 50(5), 431–442.

Sunardi, B., Sismanto, Hartantyo, E., & Nukman, M. (2025). Seismic Vulnerability In Yogyakarta Basin Based On HVSR. *International Journal of Design & Nature and Ecodynamics, 20*(4), 813–823.

Susilo, A., Juwono, A. M., Aprilia, F., Hisyam, F., Rohmah, S., Fathur, M., & Hasan, R. (2023). Subsurface Analysis Using Microtremor And Resistivity.

Widya Saputra, Y., & Azmi, M. (2024). The Use Of Andesite Rocks In Hindu-Buddhist Kingdoms In Indonesia. *Yupa: Historical Studies Journal, 8*(2), 250–262.

Xue, X., & Yang, X. (2016). Seismic Liquefaction Potential Assessed By SVM Approaches. *Bulletin of Engineering Geology and the Environment, 75*(1), 153–162.

Yulianto, T., & Yuliyanto, G. (2023). Microtremor Data And HVSR Method In The Kaligarang Fault Zone. *Data in Brief, 49*.